Ferrocene-Substituted Bis(imino)pyridine Iron and Cobalt Complexes: Toward Redox-Active Catalysts for the Polymerization of Ethylene

Vernon C. Gibson,* Nicholas J. Long,* Philip J. Oxford, Andrew J. P. White, and David J. Williams

Department of Chemistry, Imperial College London, Exhibition Road,
South Kensington, London, U.K., SW7 2AZ

Received November 8, 2005

The synthesis, characterization, and ethylene polymerization behavior of a series of iron and cobalt halide complexes $LMCl_2$ (M = Fe, Co) bearing chelating ferrocenyl-modified bis(imino)pyridyl ligands L [L = 2,6-$(FcArNCMe)_2C_5H_3N$] are reported. X-ray diffraction studies show the geometry at the metal centers to be distorted square pyramidal. Electrochemical studies focus on an Fe (**7**) and a Co (**10**) complex and in each case show several quasi-reversible oxidation and reduction waves, the ferrocenyl iron atoms being easier to oxidize than the central iron (and cobalt) atoms. Chemical oxidation of these complexes is possible via addition of $FcPF_6$, and good yields of the doubly charged iron and cobalt complexes were isolated. Treatment of the complexes **7** and **10** with methylaluminoxane (MAO) leads to highly active ethylene polymerization catalysts, converting ethylene to highly linear polyethylene (PE), with polymer molecular weights in the region of 900 000. As expected, the Fe catalyst is approximately an order of magnitude more active than the Co species, with activities of 6900 and 440 g mmol^{-1} bar^{-1} h^{-1}, respectively. The effect of the polymerization activities by oxidation of the precatalysts to their ferrocenium counterparts was seemingly negated by the reducing properties of the alkyl aluminum activator (MAO).

Introduction

The introduction of molecular polymerization catalysts has played a central role in the development of new polymeric materials. A key advantage of these new catalysts systems is the added control they afford over macromolecular properties, such as molecular weight, molecular weight distribution, comonomer incorporation, and tacticity. In recent years, complexes of the late transition metals have gained increasing prominence as olefin polymerization precatalysts.[1,2] In particular, the families of iron and cobalt catalysts bearing terdentate bis(imino)pyridine ligands have attracted great interest.[1,3−9] Here, bulky substituents on the imino nitrogen donors were found to play a pivotal role in preventing the formation of bis-chelate complexes and controlling the rates of propagation and chain termination, thus influencing both activity and molecular weight of the resultant polymer.

We have an ongoing research program that features the synthesis and characterization of redox-tunable polymerization catalyst systems probing the influence of redox-tunable ligand substituents on catalyst activities and selectivities. Previously, we[10] and others[11−14] have shown that the ferrocenyl unit can be successfully attached to the N-donor atoms of amide and imide ligands. However, we found that when positioned this close to the polymerization center, oxidation of the ferrocene units becomes problematic due to the strong electron-withdrawing effect of the pendant electrophilic metal center(s). Thus, we decided to re-focus our efforts toward ligands that are known to support polymerization active centers, but that have been modified to contain a ferrocene substituent in the ligand backbone quite remote from the active site but still within range to influence the activity and selectivity of the active center. These redox-active species offer exciting potential within homogeneous transition metal catalysts, since the oxidation of

---

* To whom correspondence should be addressed. E-mail: n.long@imperial.ac.uk; v.gibson@imperial.ac.uk. Tel: 020 75945781. Fax: 020 75945804.

[1] Gibson, V. C.; Spitzmesser, S. K. *Chem. Rev.* **2003**, *103*, 283, and references therein.

[2] Ittel, S. D.; Johnson, L. K.; Brookhart, M. *Chem. Rev.* **2000**, *100*, 1169.

[3] Gibson, V. C.; Wass, D. F. *Chem. Br.* **1999**, *7*, 20.

[4] Bennett, A. M. A. *Chemtech.* **1999**, *29*, 24.

[5] (a) Small, B. L.; Brookhart, M. *J. Am. Chem. Soc.* **1998**, *120*, 7143. (b) Britovsek, G. J. P.; Mastroianni, S.; Solan, G. A.; Baugh, S. P. D.; Redshaw, C.; Gibson, V. C.; White, A. J. P.; Williams, D. J.; Elsegood, M. R. J. *Chem. Eur. J.* **2000**, *6*, 2221.

[6] Esteruelas, M. A.; Lopez, A. M.; Mendez, L.; Olivan, M.; Onate, E. *Organometallics* **2003**, *22*, 395. Small, B. L.; Carney, M. J.; Holman, D. M.; O'Rourke, C. E.; Halfen, J. A. *Macromolecules* **2004**, *37*, 4375.

[7] Reardon, D.; Conan, F.; Gambarotta, S.; Yap, G.; Wang. Q. *J. Am. Chem. Soc.* **1999**, *121*, 9318.

[8] Tellmann, K. P.; Gibson, V. C.; White, A. J. P.; Williams, D. J. *Organometallics* **2005**, *24*, 280.

[9] (a) Britovsek, G. J. P.; Gibson, V. C.; Kimberley, B. S.; Solan, G. A.; White, A. J. P.; Williams, D. J. *Chem. Commun.* **1998**, 849. (b) Small, B. L.; Brookhart, M.; Bennett, A. M. A. *J. Am. Chem. Soc.* **1998**, *120*, 4049. (c) Britovsek, G. J. P.; Bruce, M.; Gibson, V. C.; Kimberley, B. S.; Maddox, P. J.; Mastroiani, S.; McTavish, S. J.; Redshaw, C.; Solan, G. A.; Stromberg, S.; White, A. J. P.; Williams, D. J. *J. Am. Chem. Soc.* **1999**, *121*, 8728.

[10] (a) Gibson, V. C.; Long, N. J.; Marshall, E. L.; Oxford, P. J.; White, A. J. P.; Williams, D. J. *J. Chem. Soc., Dalton Trans.* **2001**, 1162. (b) Gibson, V. C.; Halliwell, C. M.; Long, N. J.; Oxford, P. J.; Smith, A. M.; White, A. J. P.; Williams, D. J. *J. Chem. Soc., Dalton Trans.* **2003**, 918.

[11] Shafir, A.; Power, M. P.; Whitener, G. D.; Arnold, J. *Organometallics* **2001**, *20*, 1365.

[12] Siemeling, U.; Kuhnert, O.; Neumann, B.; Stammler, A.; Stammler, H. G.; Bildstein, B.; Malaun, M.; Zanello, P. *Eur. J. Inorg. Chem.* **2001**, 913.

[13] Herberhold, M. *Angew. Chem., Int. Ed.* **2002**, *41*, 956.

[14] Boer, E. J. M.; Deuling, H. H.; van der Heijden, H.; Meijboom, N.; van Oork, A. B. (Shell) WO0158874, 2001.

10.1021/om0509589 CCC: \$33.50

Scheme 1. Formation of Compounds 1−12

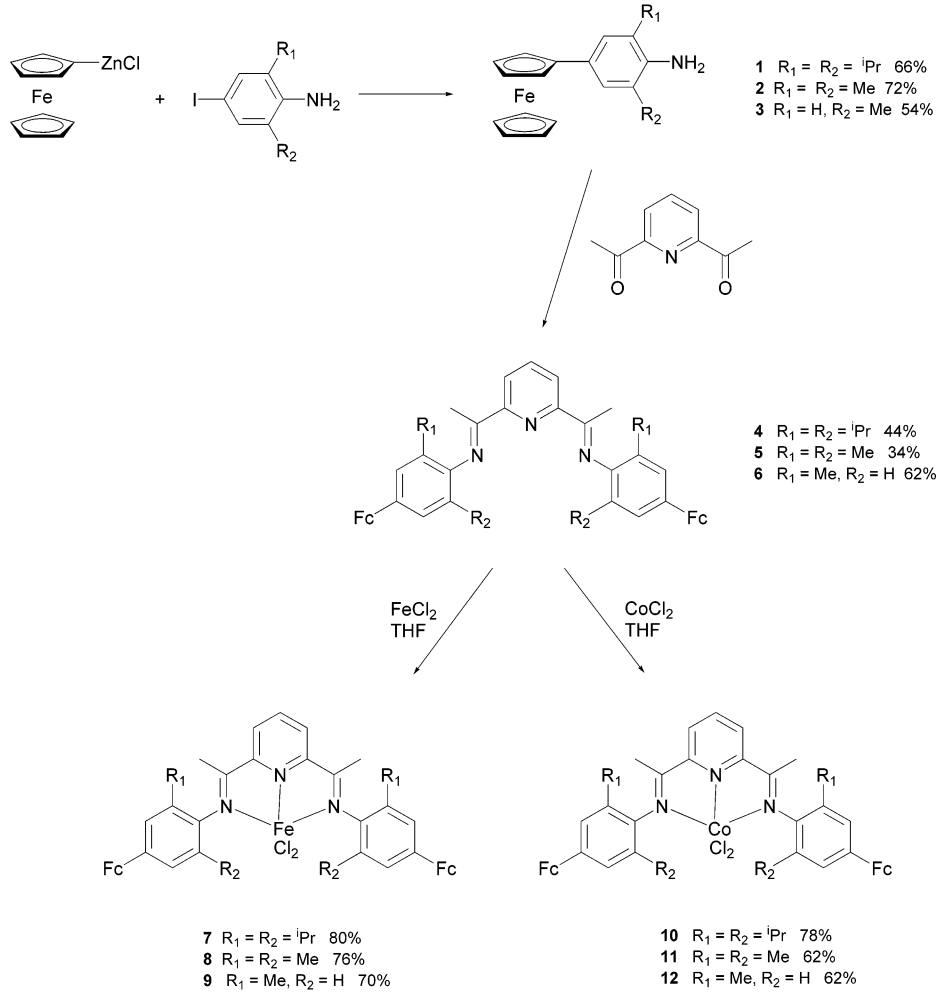

a redox-active substituent induces a higher electrophilicity and, therefore, a change in reactivity of a catalytically active transition metal center. This paper features the synthesis of new ferrocenyl-modified bis(imino)pyridine ligands, their iron and cobalt complexes, and their role as precatalysts in olefin polymerization.

Results and Discussion

The ferrocenyl anilines **1**−**3** were synthesized by the Negishi coupling reaction of ferrocenyl zinc chloride with the appropriate iodoaniline in THF solvent, using Pd(PPh_3) as a catalyst (Scheme 1). [15] The reaction mixtures were stirred at room temperature overnight to yield brown-purple solutions. The solvent was then removed under vacuum to leave dark purple oils, which were purified via column chromatography (silica gel) to give a red-colored oil (**1**) or a red waxy solid (**2** and **3**). ^{1}H NMR spectra include, in each case, a pattern of a singlet and two pseudotriplet resonances in the ferrocenyl region, which is indicative of monosubstitution of one of the Cp rings. From these precursors, the bis(imino)pyridine ligands **4**−**6** were conveniently synthesized by the condensation of the respective ferrocenyl aniline with 2,6-diacetylpyridine (Scheme 1). The reactions were carried out in refluxing ethanol, using HCl as a catalyst, and after 3 days an orange precipitate could be isolated by filtration and then recrystallized from ethanol. The new ligands were air stable and were characterized by ^{1}H and ^{13}C-{^{1}H} NMR spectroscopy, microanalysis, and FAB mass spectrometry. For example, the ^{1}H NMR spectrum of **4** shows, due to the mirror plane and the freedom of rotation of the isopropyl groups, only nine sets of resonances. Of note are the ferrocenyl resonances (a, b, c) characteristic of a monosubstituted ferrocenyl compound and the septet (e) and doublet (f) due to the isopropyl groups.

Iron dichloride complexes of the bis(imino)pyridine ligands, **7**−**9**, were formed by the reaction of a THF solution of the respective ligand with anhydrous iron(II) chloride at 60 °C for 4 h (Scheme 1). After several hours a dark green precipitate formed, which could be recrystallized from a dichloromethane/pentane (30:70) solution to give air-sensitive green crystals of **7**−**9**. The complexes formed in excellent yields, and detailed analysis was obtained for **7**, along with comparative data for **8** and **9**. Although the complexes are paramagnetic, ^{1}H NMR spectroscopy can be informative. A paramagnetic contact-shifted ^{1}H NMR spectrum was obtained for **7**, and the resonances may be assigned on the basis of integration and proximity to the paramagnetic center and by reference to literature values.[9c] The spectrum shows the ketimine protons (at −37.9 ppm), isopropyl protons (−20.6, −6.05, and −4.66 ppm), ferrocenyl protons (4.97, 5.08, and 5.32 ppm), aromatic protons (15.34 ppm), and pyridyl protons (80.99 and 81.79 ppm) (Figure 1).

X-ray diffraction quality crystals of **7** (solvated with dichloromethane) were obtained by the slow diffusion of a saturated dichloromethane solution of the complex into pentane and

---

[15] Yamamoto, A.; Morifuji, K.; Ikeda, S.; Saito, T.; Uchida, Y.; Misono, A. *J. Am. Chem. Soc.* **1968**, *90*, 1878.

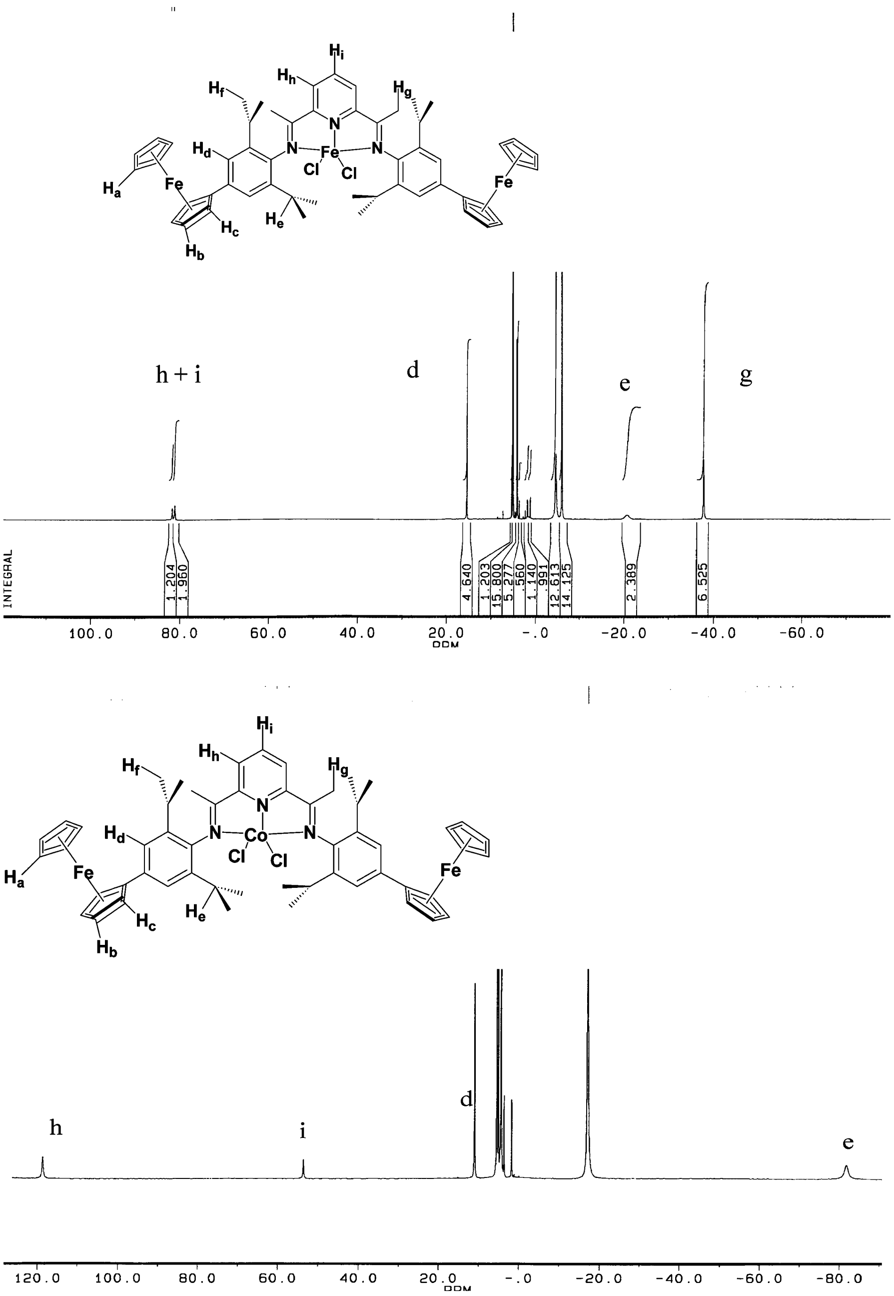

Figure 1. ^{1}H NMR spectrum and labeling of signals for **7** and **10**.

Table 1. Selected Bond Lengths (Å) and Angles (deg) for 7

Fe(1)−Cl(1)	2.3200(10)	Fe(1)−Cl(2)	2.2594(10)
Fe(1)−N(1)	2.085(3)	Fe(1)−N(7)	2.198(3)
Fe(1)−N(9)	2.207(3)	N(7)−C(7)	1.279(4)
N(9)−C(9)	1.280(4)		
Cl(1)−Fe(1)−Cl(2)	116.36(4)	Cl(1)−Fe(1)−N(1)	90.57(8)
Cl(1)−Fe(1)−N(7)	98.33(8)	Cl(1)−Fe(1)−N(9)	101.36(8)
Cl(2)−Fe(1)−N(1)	153.06(8)	Cl(2)−Fe(1)−N(7)	101.66(7)
Cl(2)−Fe(1)−N(9)	99.37(8)	N(1)−Fe(1)−N(7)	73.34(10)
N(1)−Fe(1)−N(9)	72.95(10)	N(7)−Fe(1)−N(9)	140.84(10)

isolated as green hexagonal needles. The structure of **7** is similar to that of the closely related iron complex dichloro-(2,6-bis(*N*-(2,6-diisopropylphenyl)acetylimino)pyridyl)iron(II), FECAT.[9c] The molecule has, with the exception of the two ferrocenyl substituents, approximate C_s symmetry about a plane containing the metal center, the pyridine nitrogen, and the two chlorine atoms. The orientations of the ferrocenyl units break this symmetry, both being rotated in the same sense relative to the planes of their adjacent 2,6-diisopropylphenyl rings; the torsional twists about the C(14)−C(35) and C(26)−C(45) bonds are ca. 15° and 24°, respectively. The geometry at iron is severely distorted square pyramidal, with *trans*-basal angles of 140.84(10)° [N(9),N(7)] and 153.06(8)° [N(1),Cl(2)] and axial/equatorial angles lying in the range 90.58(7)° to 116.36(4)°; the ligand *N*,*N* bite angles are 72.95(10)° and 73.34(10)°. The iron atom lies ca. 0.51 Å out of the ligand N_3 plane in the direction of Cl(1). This out-of-plane geometry is very similar to that observed in the 2,6-diisopropylphenyl structure (0.56 Å) but in striking contrast to the near-planar arrangement observed in, for example, the mesityl derivative.[9c] The Fe−N(pyridine) and Fe−Cl bond lengths in **7** (Table 1) do not differ significantly from those observed in the 2,6-diisopropylphenyl structure, though the Fe−N(imino) bonds are both ca. 0.03 Å shorter; the reason for this difference is not immediately apparent. The two ferrocenyl units have different staggered geometries with stagger angles of ca. 11° for Fe(2) and ca. 25° for Fe(3); their cyclopentadienyl rings are inclined by ca. 1° and 2°, respectively. The crystal contained two included CH_2Cl_2 solvent

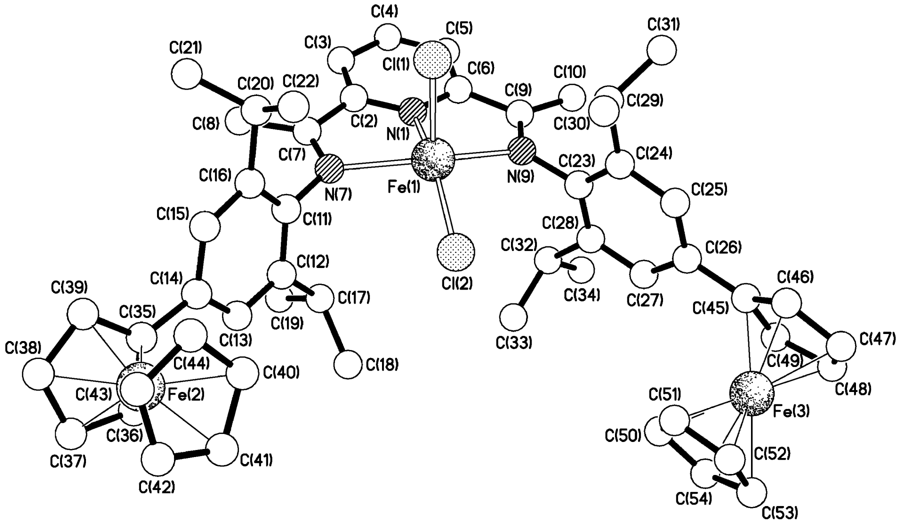

Figure 2. Molecular structure of **7**.

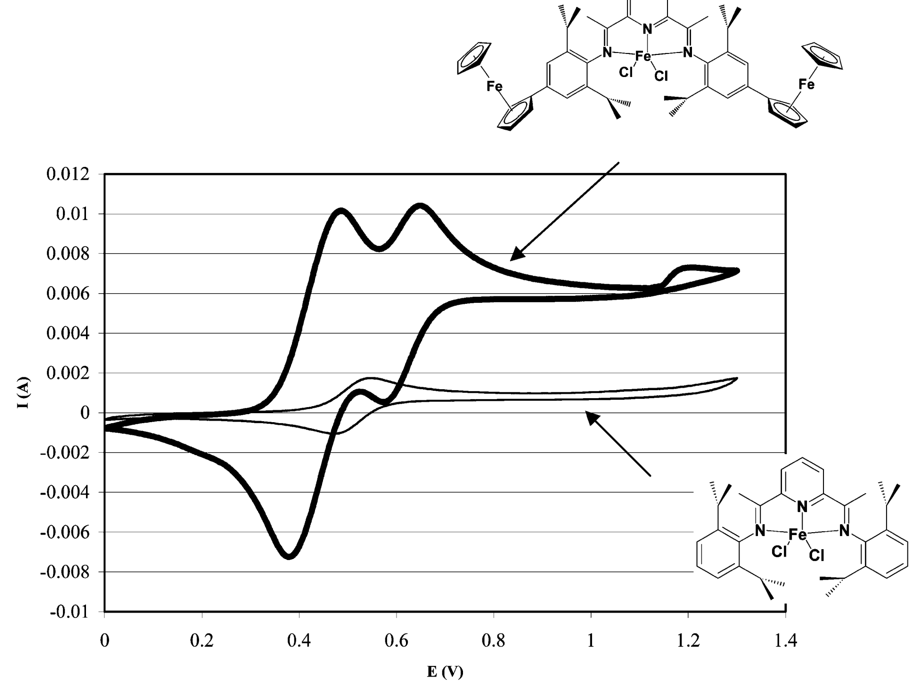

Figure 3. Comparison of the cyclic voltammograms of the iron complexes FECAT and **7**. Conditions: 0.01 M dichloromethane solution of compound; supporting electrolyte 0.1 M $^{n}Bu_4NPF_6$. Standard calomel electrode as reference electrode with palladium working and auxiliary electrodes. Scan rate 100 mV s^{-1}.

molecules, one ordered, the other disordered. There are no noteworthy packing interactions.

Cobalt(II) chloride complexes of ligands **4**−**6** could be synthesized in a fashion similar to the corresponding iron(II) complexes (Scheme 1) by stirring a mixture of ligand with anhydrous cobalt(II) chloride in THF at 60 °C for 4 h. Following filtration and washing with cold diethyl ether, the complexes **10**−**12** were isolated as red-brown solids in good yields and could be recrystallized from a dichloromethane/pentane (30:70) solution. As expected, the complexes are paramagnetic and, as for the iron analogues, a contact-shifted ^{1}H NMR spectrum was obtained for one example, compound **10**. Again the resonances were assigned on the basis of integration and proximity to the paramagnetic center and by reference to literature values.[9c] The ^{1}H NMR spectrum of **10** (Figure 1) shows isopropyl protons (at −82.8 and −17.2 ppm), the ketimine protons (1.6 ppm), aromatic protons (10.8 ppm), ferrocenyl protons (3.5, 4.2, and 4.9 ppm), and pyridyl protons (53.4 and 118.2 ppm). X-ray diffraction quality crystals of complex **10** were obtained by the slow diffusion of a saturated dichloromethane solution of **10** into pentane and isolated as red platy prisms, again with solvation by dichloromethane. The unit cell of the cobalt complex **10** was determined and found to be very similar to that of its iron analogue **7**, indicating that both the molecular and extended packing structures in the crystals of **7** and **10** are essentially the same.

Electrochemistry of Iron and Cobalt Precatalysts: Compounds 7 and 10. Due to its easily accessible and reversible one-electron redox couple (Fe(II)−Fe(III)), ferrocene is an ideal compound to study electrochemically. Substituents on the cyclopentadienyl groups affect the electron density and redox properties of the ferrocenyl iron center. Herein, the effect on the central iron(II) or cobalt(II) centers by the ferrocene-substituted bis(imino)pyridine ligand is examined for **7** and **10** and

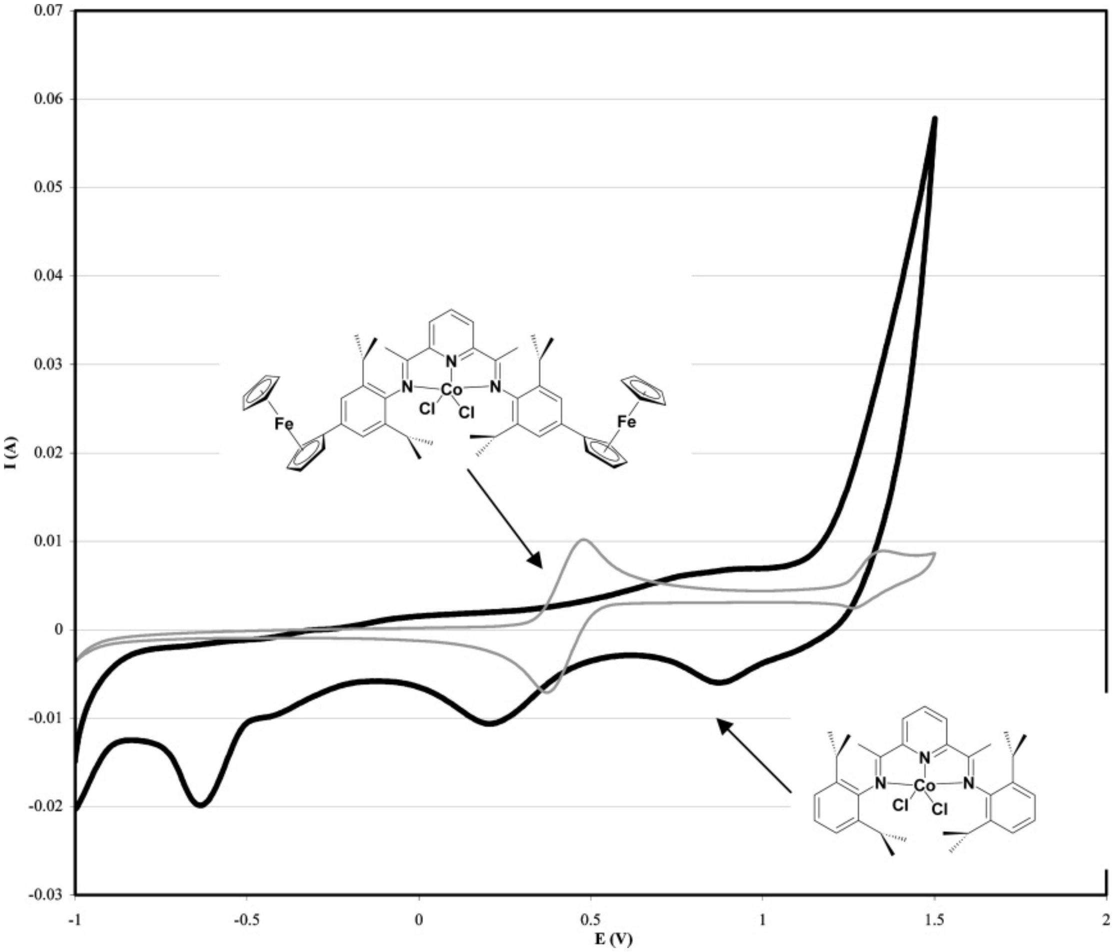

Figure 4. Cyclic voltammetry of the cobalt complexes COCAT and **10**. Conditions: 0.01 M dichloromethane solution of compound; supporting electrolyte 0.1 M $^{n}Bu_4NPF_6$. Standard calomel electrode as reference electrode with palladium working and auxiliary electrodes. Scan rate 100 mV s^{-1}.

Table 2. Cyclic Voltammetry of Bis(imino)pyridine Compounds

complex	$E_p^a(1)$ (V)	$E_p^c(1)$ (V)	$E_{1/2}(1)$ (V)	$E_p^a(2)$ (V)	$E_p^c(2)$ (V)	$E_{1/2}(2)$ (V)	$E_p^c(3)$ (V)
ferrocene	0.470	0.360	0.405				
FECAT	0.550	0.473	0.512				
7	0.488	0.378	0.433	0.644	0.574	0.609	
COCAT		0.874			0.200		−0.624
10	0.484	0.373	0.429				

their well-known and catalytically active non-ferrocenyl counterparts **FECAT** and **COCAT**. The cyclic voltammograms are shown as Figures 3 and 4, and results are tabulated in Table 2.

For compound **7**, two oxidation and reduction waves are observed. The initial oxidation is attributed to the ferrocenyl groups and has a half-potential of 0.433 V. The second wave is due to the quasi-reversible, one-electron transfer for the Fe(II)−Fe(III) redox couple of the central iron atom, with a half-potential of 0.609 V. In comparison to FECAT the oxidation potential is shifted by 0.907 V. The ferrocenyl iron atoms are therefore easier to oxidize than the central iron atom, and the resulting positive charge means that the central iron atom is harder to oxidize. Oxidation of the ferrocenyl moieties therefore changes the electron potential at the central iron atom, and its effect on polymerization may be observed (see later). In comparison, the cobalt complexes show a different pattern (Figure 3). The main feature of the cyclic voltammogram of **10** is the single quasi-reversible Fe(II)−Fe(III) wave of the ferrocenyl substituents with a half-potential of 0.429 V. There is possibly a further oxidation at 1.2 V, but this is at the limit of the solvent window, and full electrochemical information could not be obtained. In contrast the unsubstituted cobalt complex COCAT shows three reduction peaks at 0.874, 0.200, and −0.624 V. The reduction peaks have been tentatively assigned to Co(III), Co(III)−Co(II), and Co(II)−Co(I) (Table 2).

Although the cyclic voltammetry studies show that the oxidation potentials of the ferrocenyl units of the iron and cobalt complexes are higher than that of ferrocene, the chemical oxidation of complexes **7** and **10** was easily carried out by the addition of 2 equiv of ferrocenium hexafluorophosphate in dichloromethane solution (Scheme 2). The reaction was stirred at 40 °C for 2 h. A color change of green to khaki was noted for the iron complex **13** and from orange-brown to khaki-brown for the cobalt complex **14**. The solvent was removed in vacuo, and the resulting crude solid was further heated under vacuum, during which time orange crystals of ferrocene were seen to sublime in the Schlenk tube. The solids were washed with pentane, dried, and isolated in yields of 46% for **13** and 64% for **14**. The ferrocenium salts were insoluble in most organic solvents and were metastable in air. They were stored under dry nitrogen. Characterization (FAB MS and microanalysis)

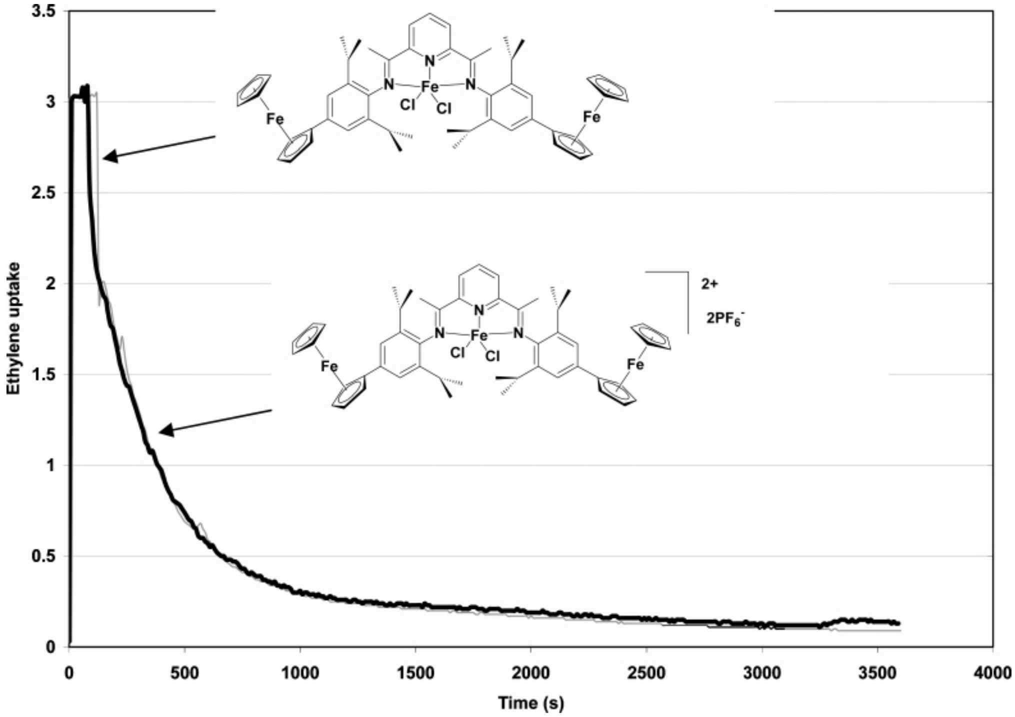

Figure 5. Reactivity profiles for ethylene polymerization in stainless steel reactor vessel.

Scheme 2

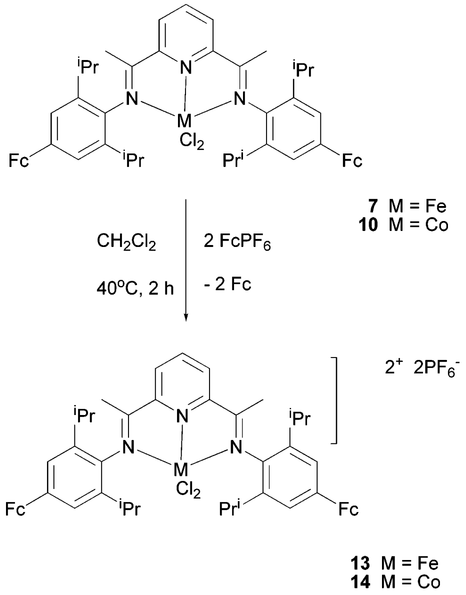

Table 3. Summary of Reactor Trials for Ethylene Polymerization

catalyst	catalyst (μmol)	MAO (μmol)	effective ratio MAO:cat.	mass of polymer (g)	activity (g mmol^{-1} bar^{-1} h^{-1})
FECAT	1	100	4100:1	23.5	5875
7	1	100	4100:1	27.6	6900
13	1	100	4100:1	27.4	6850
10	4	400	4100:1	7.1	440
COCAT	4	400	4100:1	10.0	630

confirmed that **13** and **14** were the dicationic bis-hexafluorophosphate salts.

Ethylene Polymerization Studies. The ethylene polymerization activity of the iron and cobalt precatalysts **7** and **10** was been evaluated in a double-jacketed, 1 L stainless steel autoclave. Polymerization was commenced by injection of a toluene solution of activated catalyst at a constant pressure of ethylene (4 bar). The results of the tests are given in Table 3, and the reaction profiles are illustrated in Figure 5. Precatalysts FECAT and COCAT were also tested in order to compare the effects of the ferrocenyl groups. The nature of the metal center has a large influence on catalyst productivity. It can be seen that the iron catalysts show a larger activity (by about an order of magnitude) than their cobalt equivalents, and this is the same trend seen for the non-ferrocenyl analogues.[9c] A modest increase in activity is seen for **7** relative to the non-ferrocenyl FECAT precatalyst. which may reflect the greater electron-withdrawing capacity of the ferrocenyl unit and in turn would lead to an increase in electrophilicity of the catalytically active iron center. However, this is not seen for the cobalt system, where a decrease in activity is found for **10** versus COCAT.

Molecular weight data for **7** and **10** reveal M_w values of 865 000 and 19 000, respectively, with a molecular weight distribution for the iron catalyst of 15.3 and 3.8 for the cobalt system. These values are typical of bis(imino)pyridine iron and cobalt catalysts.[9] Interestingly, the oxidation of the ferrocene moieties appears to have little or no effect on the catalyst activity since the reactivity profile and activity of the ferrocene (**7**) and ferrocenium (**13**) species are almost identical. Further, the M_w of the resultant polyethylene using **13**, 942 000 (PDI 11.1), is virtually identical to that obtained using **7**. This suggests that the dicationic ferrocenium species is likely reduced by the alkylaluminum cocatalyst. In this context, reduction of Fe(III) to Fe(II) species by alkyl aluminum compounds has been documented.[15] To test this hypothesis, a sample of ferrocenium hexafluorophosphate was treated with MAO. The blue-colored solution immediately turned green and, on stirring, turned orange; it was possible to isolate ferrocene from the reaction mixture. Thus, to see any effect of ferrocene acting as a redox switch for ethylene polymerization, a system free of MAO will be required. Systems amenable to the stabilization of cationic alkyl species using weakly coordinating anions are expected to be more suited to this requirement.

Conclusions

The synthesis and characterization of a family of iron- and cobalt-based ethylene polymerization precatalysts featuring ferrocenyl substituents have been described. As with the non-ferrocenyl analogues, activation with MAO produces highly active catalysts with the iron species being an order of magnitude more active than the Co species.

As expected, the ferrocene-substituted complexes show a rich electrochemistry, featuring quasi-reversible processes, though it has not proved possible to establish the effect on the catalytic activities of the oxidized precatalysts due to the reducing properties of the activator. Thus, further work is underway to understand more fully the role and influence of the ferrocenyl substituents, particularly their use in catalytic systems that do not require alkyl aluminum activators.

Experimental Section

General Details. All preparations were carried out under an atmosphere of nitrogen using standard Schlenk techniques or an inert atmosphere (nitrogen) glovebox, unless otherwise stated. All solvents were distilled over standard drying agents under nitrogen directly before use and deoxygenated. Silica gel (Kieselgel grade 60) was used for chromatographic separations. All NMR spectra were recorded using a Delta upgrade on a JEOL EX270 MHz spectrometer. Chemical shifts are reported in δ (ppm) using residual proton impurities in $CDCl_3$ (^1H δ 7.25 ppm, ^{13}C δ 77.0 ppm) or CD_2Cl_2 (^1H δ 5.32 ppm, ^{13}C δ 53.8 ppm) as the reference solvent. Mass spectra were recorded using positive FAB methods for organometallic compounds, and EI for organic compounds, on a micromass Autospec spectrometer (primary ion beam 35 keV Cs^+ and 3-nitrobenzyl alcohol matrix) by Mr. J. Barton, Imperial College. Microanalyses were carried out by Mr. S. Boyer of the London Metropolitan University.

Polyethylene analysis was performed at BP Chemicals Limited by J. Boyle (NMR) and G. Audley (GPC). GPC traces were recorded using PL gel 2 x mixed bed-D, 30 cm, 5 μm columns, trichlorobenzene eluent, and a flow rate of 1.0 mL/min at 150 °C using a refractive index detector. Starting materials were prepared according to adapted literature procedures (referenced where appropriate) and were characterized by ^1H NMR and ^{13}C NMR and mass spectrometry where appropriate. All other chemicals were purchased from commercial sources and used without further purification unless stated. Research grade ethylene (BOC) was used for all ethylene polymerization experiments. Methyl aluminoxane (MAO) was obtained as a 1.6 M solution in toluene. 4-Fc-2,6-diisopropylaniline (**1**) was prepared using the method of Siemeling,[16] and NaBAF, [17] FcBA,[18] FECAT,[9] and COCAT[9] were prepared using literature procedures.

Synthesis of 4-Ferrocenyl-2,6-dimethylaniline (2). A procedure analogous to that described by Siemeling[16] for **1** was followed but using iodo-2,6-dimethylaniline to yield **2** (72%) as an waxy red solid. ^1H NMR ($CDCl_3$, ppm): 2.21(s, 6H, CH_3), 3.54 (br s, 2H, NH_2), 4.04 (s, 5H, C_5H_5), 4.22 (t, 2H, C_5H_4), 4.52 (t, 2H, C_5H_4), 7.08 (s, 2H, C_6H_2). FAB MS (+ve): *m*/*e* 304 $[M]^+$.

Synthesis of 4-Ferrocenyl-2-methylaniline (3). A procedure analogous to that described by Siemeling[16] for **1** was followed but using 1-iodo-2-methylaniline to yield **3** (54%) as a waxy red solid. ^1H NMR ($CDCl_3$, ppm): 2.21(s, 3H, CH_3), 3.57 (br s, 2H, NH_2), 4.04 (s, 5H, C_5H_5), 4.23 (t, 2H, C_5H_4), 4.54 (t, 2H, C_5H_4), 6.63 (multiplet, 1H, C_6H_3), 7.20 (multiplet, 2H, C_6H_3). FAB MS (+ve): *m*/*e* 290 $[M]^+$.

2,6-Diacetylpyridinebis(4-ferrocenyl-2,6-diisopropylaniline) (4). To a solution of 2,6-diacetylpyridine (0.74 g, 4.5 mmol) in absolute ethanol (50 mL) was added 4-Fc-2,6-diisopropylaniline (3.30 g, 9.1 mmol). The mixture was purged with nitrogen for 10 min. After the addition of 2 drops of glacial acetic acid the mixture was refluxed for 5 days, during which time an orange precipitate had formed. The reaction mixture was cooled to room temperature and filtered. The filtrate was washed with cold ethanol and dried to give **4** (1.70 g, 44%). ^1H NMR ($CDCl_3$, ppm): 1.20 (d, 24H, $^3J_{H-H} = 3.3$ Hz, $CHMe_2$), 2.31 (s, 6H, CH_3), 2.79 (sept, 4H, $^3J_{H-H} = 3.3$ Hz, $CHMe_2$), 4.07 (s, 10H, C_5H_5), 4.29 (t, 4H, C_5H_4), 4.63 (t, 4H, C_5H_4), 7.30 (s, 4H, C_6H_2), 7.94 (t, 1H, $^3J_{H-H} = 3.8$ Hz, C_5H_3-py), 8.5 (d, 2H, C_5H_3-py). ^{13}C NMR ($CDCl_3$, ppm): 17.2 ($CHMe_2$), 23.4 ($CHMe_2$), 28.2 ($N{=}CMe$), 66.6 (C_5H_5-Cp), 68.3 (C_5H_4-Cp), 69.5 (C_5H_4-Cp), 87.5 (*ipso*-C C_5H_4-Cp), 121.4 (C_6H_2), 122.1 (C_5H_3-py), 133.8 (C_5H_3-py), 135.6 (C_6H_2), 136.9 (C_6H_2), 155.2 (C_6H_2), 161.8 (C_5H_3-py), 167.1 ($N{=}C$). FAB MS (+ve): *m*/*e* 849 $[M]^+$. Anal. Calcd for $C_{53}H_{59}Fe_2N_3$: C, 74.91; H, 6.95; N, 4.94. Found: C, 74.78; H, 7.15; N, 4.82.

2,6-Diacetylpyridinebis(4-ferrocenyl-2,6-dimethylaniline) (5). A procedure analogous to that described for **4** was followed but using 2,6-diacetylpyridine (0.25 g, 1.6 mmol) and 4-ferrocenyl-2,6-dimethylaniline (1.0 g, 3.2 mmol) to yield **5** (0.41 g, 34%). ^1H NMR ($CDCl_3$, ppm): 2.06 (s, 12H, CH_3), 2.28 (s, 6H, CH_3), 4.08 (s, 10H, C_5H_5), 4.21 (t, 4H, C_5H_4), 4.62 (t, 4H, C_5H_4), 7.20 (s, 4H, C_6H_2), 7.93 (t, 1H, $^3J_{H-H} = 3.8$ Hz, C_5H_3-py), 8.50 (d, 2H, C_5H_3-py). ^{13}C NMR ($CDCl_3$, ppm): 16.6 (Ar-*Me*), 18.1 ($N{=}CMe$), 66.1 (C_5H_5-Cp), 68.4 (C_5H_4-Cp), 69.5 (C_5H_4-Cp), 86.0 (*ipso*-C C_5H_4-Cp), 122.2 (C_6H_2), 122.4 (C_5H_3-py), 125.8 (C_6H_2), 133.5 (C_6H_2), 136.8 (C_6H_2), 147.0 (C_5H_3-py), 155.2 (C_5H_3-py), 167.3 ($N{=}C$). FAB MS (+ve): *m*/*e* 737 $[M]^+$. Anal. Calcd for $C_{45}H_{43}Fe_2N_3$: C, 73.27; H, 5.83; N, 5.69. Found: C, 73.16; H, 6.04; N, 5.48.

2,6-Diacetylpyridinebis(4-ferrocenyl-2-methylaniline) (6). A procedure analogous to that described for **4** was followed but using 2,6-diacetylpyridine (0.55 g, 3.4 mmol) and 4-ferrocenyl-2-methylaniline (2.0 g, 6.85 mmol) to yield **6** (1.51 g, 62%). ^1H NMR ($CDCl_3$, ppm): 2.17 (s, 6H, CH_3), 2.41 (s, 6H, CH_3), 4.07 (s, 10H, C_5H_5), 4.30 (t, 4H, C_5H_4), 4.64 (t, 4H, C_5H_4), 6.6 (m, 2H, C_6H_3), 7.33 (m, 4H, C_6H_3), 7.92 (t, 1H, $^3J_{H-H}$ 3.8, C_5H_3-py), 8.40 (d, 2H, C_5H_3-py). ^{13}C NMR ($CDCl_3$, ppm): 16.4 (Ar-*Me*), 17.9 ($N{=}CMe$), 66.1 (C_5H_5-Cp), 68.6 (C_5H_4-Cp), 69.5 (C_5H_4-Cp), 85.8 (*ipso*-C C_5H_4-Cp), 118.3 (C_6H_3), 122.2 (C_5H_3-py), 123.6 (C_6H_3), 124.2 (C_6H_3), 127.3 (C_6H_3), 128.0 (C_6H_3), 134.2 (C_6H_3), 147.9 (C_5H_3-py), 155.4 (C_5H_3-py), 166.8 ($N{=}C$). FAB MS (+ve): *m*/*e* 709 $[M]^+$. Anal. Calcd for $C_{43}H_{39}Fe_2N_3\cdot 1.25CH_2Cl_2$: C, 65.15; H, 5.09; N, 5.15. Found: C, 65.00; H, 5.04; N, 4.92.

(2,6-Diacetylpyridinebis(4-ferrocenyl-2,6-diisopropylaniline))-$FeCl_2$ (7). A solution of **4** (0.8 g, 0.94 mmol) in THF (30 mL) was added to a solution of $FeCl_2$ (0.12 g, 0.94 mmol) also in THF (30 mL) to yield a dark green solution. The mixture was stirred for 4 h, during which time a dark green solid had precipitated. The mixture was filtered and the residual green solid washed with cold diethyl ether (2 × 10 mL). The solid was dried to give a dark green powder (0.74 g, 80%). ^1H NMR (CD_2Cl_2 broad signals observed, ppm): −37.9 (6H, $N{=}C(Me)$), −20.6 (4H, $CH(CH_3)_2$), −6.05 (12H, $CH(CH_3)_2$), −4.66 (12H, $CH(CH_3)_2$), 4.97 (4H, C_5H_4-Cp), 5.08 (10H, C_5H_5-Cp), 5.32 (4H, C_5H_4-Cp), 15.34 (4H, Ar-H_m), 80.98 (1H, py-H_p), 81.79 (2H, py-H_m). FAB MS (+ve): *m*/*e* 975 $[M]^+$. Anal. Calcd for $C_{53}H_{59}Cl_2Fe_3N_3$: C, 65.16; H, 6.04; N, 4.30. Found: C, 64.92; H, 5.93; N, 4.20.

(2,6-Diacetylpyridinebis(4-ferrocenyl-2,6-dimethylaniline))-$FeCl_2$ (8). A procedure analogous to that described for **7** was followed but using **5** (0.08 g, 0.1 mmol) and $FeCl_2$ (0.012 g, 0.01 mmol) to yield **8** (0.07 g, 76%). ^1H NMR (CD_2Cl_2 broad signals observed, ppm): −26.27 (6H, $N{=}C(Me)$), 4.61 (10H, C_5H_5-Cp),

---

(16) Siemeling, U.; Neumann, B.; Stammler, H.-G.; Kuhnert, O. *Polyhedron* **1999**, *18*, 1815.

(17) Brookhart, M.; Grant, B.; Volpe, A. F. *Organometallics* **1992**, *11*, 3920.

(18) Heinekey, D. M.; Radzewich, C. E. *Organometallics* **1998**, *17*, 51.

4.81 (4H, C_5H_4-Cp), 5.32 (4H, C_5H_4-Cp), 12.84 (12H, Ar-C*H*$_3$), 16.88 (4H, Ar-H_m), 35.27 (1H, py-H_p), 82.38 (2H, py-H_m). FAB MS (+ve): *m*/*e* 863 [M]$^+$. Anal. Calcd for $C_{45}H_{43}Cl_2Fe_3N_3$: C, 62.51; H, 4.97; N, 4.86. Found: C, 62.49; H, 5.03; N, 4.85.

(2,6-Diacetylpyridinebis(4-ferrocenyl-2-methylaniline))-$FeCl_2$ (9). A procedure analogous to that described for **7** was followed but using **6** (0.23 g, 0.32 mmol) and $FeCl_2$ (0.04 g, 0.31 mmol) to yield **9** (0.19 g, 70%). FAB MS (+ve): *m*/*e* 835 [M]$^+$. Anal. Calcd for $C_{43}H_{39}Cl_2Fe_3N_3$: C, 61.70; H, 4.66; N, 5.02. Found: C, 61.69; H, 4.72; N, 4.85.

(2,6-Diacetylpyridinebis(4-ferrocenyl-2,6-diisopropylaniline))-$CoCl_2$ (10). A solution of **4** (0.40 g, 0.47 mmol) in 30 mL of THF was added to a solution of $CoCl_2$ (0.06 g, 0.47 mmol) also in THF (30 mL) to yield a red-brown solution. The mixture was stirred for 4 h, during which time a dark brown solid had precipitated. The mixture was filtered and the residual brown solid washed with cold diethyl ether (2 × 10 mL). The solid was dried to give a red-brown powder (0.35 g, 78%). ^{1}H NMR (CD_2Cl_2, ppm): −82.8 (6H, C*H*(CH_3)$_2$), −17.2 (12H, CH(C*H*$_3$)$_2$), 1.6 (6H, N=C(*Me*)), 3.5 (4H, C_5H_4-Cp), 4.2 (5H, C_5H_5-Cp), 4.9 (4H, C_5H_4-Cp), 10.8 (4H Ar-H_m), 53.4 (1H, py-H_p), 118.2 (2H, py-H_m). FAB MS (+ve): *m*/*e* 978 [M]$^+$. Anal. Calcd for $C_{53}H_{59}Cl_2CoFe_2N_3$: C, 64.96; H, 6.02; N, 4.29. Found: C, 64.85; H, 5.81; N, 4.12.

(2,6-Diacetylpyridinebis(4-ferrocenyl-2,6-dimethylaniline))-$CoCl_2$ (11). A procedure analogous to that described for **10** was followed but using **5** (0.55 g, 0.77 mmol) and $CoCl_2$ (0.10 g, 0.71 mmol) to yield **11** (0.40 g, 62%). FAB MS (+ve): *m*/*e* 865 [M]$^+$. Anal. Calcd for $C_{45}H_{43}Cl_2CoFe_2N_3$: C, 62.35; H, 4.96; N, 4.85. Found: C, 62.13; H, 4.99; N, 4.62.

(2,6-Diacetylpyridinebis(4-ferrocenyl-2-methylaniline))-$CoCl_2$ (12). A procedure analogous to that described for **10** was followed using **6** (0.23 g, 0.32 mmol) and $CoCl_2$ (0.04 g, 0.31 mmol) to yield **12** (0.17 g, 62%). FAB MS (+ve): *m*/*e* 837 [M]$^+$. Anal. Calcd for $C_{43}H_{39}Cl_2CoFe_2N_3$: C, 61.59; H, 4.59; N, 4.97. Found: C, 61.52; H, 4.65; N, 5.00.

(2,6-Diacetylpyridinebis(4-ferrocenium-2,6-diisopropylaniline))-$FeCl_2$ $(PF_6)_2$ (13). To a suspension of ferrocenium hexafluorophosphate (0.12 g, 0.36 mmol) in dichloromethane (25 mL) was added a solution of **7** (0.17 g, 0.18 mmol) in dichloromethane. The mixture was stirred for 4 h, and the volatiles were removed in vacuo. The resulting green solid was washed with pentane (25 mL) and dried to yield **13** (0.21 g 46%). FAB MS (+ve): *m*/*e* 1120 [M − PF_6]$^+$. Anal. Calcd for $C_{53}H_{59}Cl_2Fe_3N_3P_2F_{12}$: C, 50.20; H, 4.66; N, 3.32. Found: C, 50.17; H, 4.54; N, 3.19.

(2,6-Diacetylpyridinebis(4-ferrocenium-2,6-diisopropylanil))-$CoCl_2(PF_6)_2$ (14). A procedure analogous to that described for **13** was followed but using ferrocenium hexafluorophosphate (0.07 g, 0.21 mmol) and **10** (0.1 g, 0.11 mmol) to yield **14** (0.09 g, 64%). FAB MS (+ve): *m*/*e* 1123 [M − PF_6]$^+$. Anal. Calcd for $C_{53}H_{59}Cl_2CoFe_2N_3P_2F_{12}$: C, 50.10; H, 4.60; N, 3.31. Found: C, 49.60; H, 5.00; N, 2.85.

Crystal data for 7: $C_{53}H_{59}N_3Cl_2Fe_3{\cdot}2CH_2Cl_2$, $M = 1146.33$, monoclinic, $P2_1/c$ (no. 14), $a = 18.501(2)$ Å, $b = 13.7329(12)$ Å, $c = 21.937(2)$ Å, $\beta = 91.093(9)°$, $V = 5572.5(9)$ Å^3, $Z = 4$, $D_c = 1.366$ g cm^{-3}, μ(Mo Kα) = 1.096 mm^{-1}, $T = 203$ K, green hexagonal needles; 9771 independent measured reflections, F^2 refinement, $R_1 = 0.046$, $wR_2 = 0.107$, 7405 independent observed absorption-corrected reflections [$|F_o| > 4\sigma(|F_o|)$, $2\theta_{max} = 50°$], 616 parameters. CCDC 600245.

Crystal data for 10: $C_{53}H_{59}N_3Cl_2Fe_2Co{\cdot}2CH_2Cl_2$, $M = 1149.41$, monoclinic, $P2_1/c$ (no. 14), $a = 18.527(2)$ Å, $b = 13.7570(14)$ Å, $c = 21.911(2)$ Å, $\beta = 91.063(9)°$, $V = 5583.7(12)$ Å^3, $Z = 4$, $D_c = 1.370$ g cm^{-3}, μ(Mo Kα) = 1.133 mm^{-1}, $T = 203$ K, red platy prisms (only unit cell determined).

Cyclic Voltammetry. In all cases measurements were performed using an Autolab PGSTAT12 potentiometer with Gpes software, with 0.1 M tetrabutylammonium-hexafluorophophate as the electrolyte in dichloromethane. The sample solution was approximately 1 mM concentration in this electrolyte. The working electrode was platinium, circular and 1 mm in diameter, the reference was an Ag/AgCl electrode, and the counter electrode was a platinum wire. The cyclic voltammograms were measured at rates of 100 mV s^{-1} and the potentials calculated using ferrocene as a comparison.

Ethylene Polymerization Tests. A solution of the catalyst was introduced to the reactor though the injector unit by an overpressure of nitrogen. Constant ethylene pressure was maintained throughout the reaction via a pressure regulator connected to a mass flow controller, and constant temperature was maintained by the circulation of thermostatically controlled oil. The ethylene flow rate, polymerization temperature, and autoclave pressure were all logged by computer. For a polymerization test the reactor was first heated to 85 °C for 1 h under a continuous flow of nitrogen, to remove atmospheric oxygen and moisture. The reactor was cooled to reaction temperature (50 °C) and the isobutane solvent (0.5 l) added. An oxygen/moisture scavenger (MAO) was added to the reactor followed by the desired pressure of ethylene and the solvent/scavenger mix stirred for 30 min. The test was terminated by venting of the volatile components. The reactor contents were isolated, washed with aqueous hydrochloric acid in methanol, and dried under vacuum.

Acknowledgment. The Department of Chemistry, Imperial College London, is thanked for a Teaching Assistantship (for P.J.O.), and BP Amoco Chemicals Ltd. is thanked for GPC measurements and analysis.

OM0509589